Paraconductivity and excess Hall conductivity in $YBa_2Cu_3O_{7-x}/PrBa_2Cu_3O_{7-x}$ superlattices

L. M. Wang and H. C. Yang
Department of Physics, National Taiwan University, Taipei 10764, Taiwan, Republic of China

H. E. Horng
Department of Physics, National Taiwan Normal University, Taipei 11718, Taiwan, Republic of China

(Received 30 June 1998; revised manuscript received 11 December 1998)

The paraconductivities and excess Hall conductivities of $YBa_2Cu_3O_{7-x}$ (YBCO) films and $YBa_2Cu_3O_{7-x}/PrBa_2Cu_3O_{7-x}$ (YBCO/PBCO) superlattices at temperatures above T_c are measured and analyzed within the framework of fluctuation theories. We observe that the fluctuation contributions to the paraconductivity of YBCO/PBCO superlattices are governed by the Lawrence and Doniach process and the dimensionality is characterized by the coupling parameter α, which is temperature dependent. However, the contributions of fluctuation to the excess Hall effect contain the negative Aslamazov-Larkin (AL) term and the positive Maki-Thompson (MT) term. Especially, the positive MT contributions for YBCO/PBCO superlattices suggest that the pair-breaking interaction is important when T is close T_c. The scaling of the paraconductivities in the presence of magnetic fields suggests that the YBCO/PBCO superlattices belong to the quasi-two-dimensional (quasi-2D) systems and the anisotropic parameter $\gamma = m_{ab}/m_c$ governs the dimensionality. With a smaller value of γ, a 2D-like scaling of the paraconductivities is obtained. On the other hand, in the scaling of the excess Hall conductivities, only the AL terms separated from the total conductivities follow a scaling law, while the MT terms do not. The results are discussed. [S0163-1829(99)05121-8]

I. INTRODUCTION

One of the important features of the high-T_c superconductors is the large fluctuation occurring at temperatures well above the mean-field transition temperature. The layered high-T_c superconductors have a relatively large fluctuation region due to their short coherence lengths and high transition temperatures T_c. Effects of superconducting fluctuations have been seen in various properties of high-T_c superconductors, including electrical conductivity,[1–5] specific heat,[6] magnetic susceptibility,[4,7] magnetoresistance,[5,8] and the Hall effect.[1–3] Additionally, though the study of fluctuation effects in superconductors has a long history, new theoretical models for fluctuation effects are currently in development.[9,10]

The investigation of fluctuation-induced conductivity is regarded as a way to probe the dimensionality of the order-parameter fluctuation. Based on the Aslamazov-Larkin[11] (AL) and Maki-Thompson[12] (MT) theories, the measurements of fluctuation conductivities on high-T_c superconductors suggest they involve a crossover from two-dimensional (2D) to 3D for $YBa_2Cu_3O_{7-x}$ (YBCO) (Ref. 13) and 2D characteristics for the Bi-Sr-Ca-Cu-O (Ref. 14) and Tl-Ba-Ca-Cu-O (Ref. 15) systems. Similarly, several scaling theories[16–18] have also been applied to explain the excess conductivities in the fluctuation region.

On the other hand, there is an anomalous sign reversal of the Hall coefficient in the mixed state of both high-T_c and low-T_c superconductors. Recently, Li, Zhang, and Adrian[19] as well as Wang, Yang, and Horng[20] reported the effect of flux pinning on the mixed-state Hall coefficient in YBCO/$PrBa_2Cu_3O_{7-x}$ (PBCO) superlattices. In addition, Liu *et al.*[21] measured the longitudinal and Hall resistive transitions of YBCO films, concluding that the AL term dominates the MT term, therefore causing a sign change of total Hall conductivity at temperatures above $T_c(H)$. Apparently, an interesting question at issue is whether the sign change is due to the large negative fluctuation of Hall conductivity or the intrinsic property of vortex dynamics. This is a topic of current interest.

In this work, the high-T_c superconducting YBCO/PBCO superlattices were prepared to study the fluctuation phenomena. Superconducting YBCO/PBCO superlattices were *in situ* grown onto rotated $SrTiO_3(001)$ substrates in a rf magnetron sputtering system. The sample preparation and the transport measurement have been in detail described elsewhere.[22] The YBCO/PBCO superlattices offer the possibility to control the coupling along the *c* direction between the neighboring superconducting layers. By modifying the thickness of the semiconducting PBCO layers and superconducting YBCO layers, one can change the coupling length and therefore the anisotropy of the system. The measurements of excess conductivity in a series of YBCO/PBCO superlattices provide us with a good opportunity to examine the predictions of fluctuation theories. This work reports on the excess Hall conductivities and scaling behaviors of fluctuation conductivities in fields for YBCO/PBCO superlattices.

II. THEORETICAL BACKGROUND

A. Paraconductivity

The paraconductivity $\Delta\sigma_{xx}$ has been most extensively studied in the layered-structure systems for the enhancement of conductivity. Aslamazov and Larkin[11] pointed out that thermal fluctuations in a superconductor result in a finite probability of a Cooper pair formation above T_c, leading to

an excess electrical conductivity for $T>T_c$. The fluctuation-enhanced conductivity is given by

$$(\Delta\sigma_{xx}^{\mathrm{AL}})_{3\mathrm{D}}=\frac{e^2}{32\hbar}\frac{1}{\xi(0)}\varepsilon^{-1/2} \tag{1}$$

and

$$(\Delta\sigma_{xx}^{\mathrm{AL}})_{2\mathrm{D}}=\frac{e^2}{16\hbar}\frac{1}{d}\varepsilon^{-1}, \tag{2}$$

where $\xi(0)$ is the coherence length at zero temperature, $\varepsilon=\ln(T/T_c)\approx(T-T_c)/T_c$, and d is the characteristic length of the 2D system (i.e., the film thickness in superconducting films or the distance between adjacent layers in the layered superconductors). In order to express the 2D-3D crossover regime [$\xi_c(T)\sim d/2$], Lawrence and Doniach[23] (LD) modeled layered superconductors as stacks of 2D superconducting layers, weakly coupled by Josephson tunneling. This expression, which depends on the dimensionality of the sample, has been extended for 2D-like, layered high-T_c superconductors. The paraconductivity in the LD model is given by

$$\Delta\sigma_{xx}^{\mathrm{LD}}=\frac{e^2}{16\hbar d}(1+2\alpha)^{-1/2}\varepsilon^{-1}, \tag{3}$$

where d is the distance between adjacent layers and α is the coupling parameter:

$$\alpha=\frac{2\xi_c^2(T)}{d^2}=\frac{2\xi_c^2(0)}{d^2\varepsilon}. \tag{4}$$

This models the crossover from the 2D limit at high temperature to the 3D behavior as the temperature-dependent coherence length $\xi_c(T)$ along the stacking direction exceeds the layer distance at temperature near T_c. In other words, Eq. (3) would be reduced to the 2D AL form [Eq. (2)] for $T\gg T_c$ [$\xi_c(T)\ll d$], to the 3D AL form [Eq. (1)] for $T\sim T_c$ ($\xi_c\gg d$), and it exhibits a 2D-3D crossover at $T^*\approx T_c\{1+[2\xi_c(0)/d]^2\}$ [i.e., $\xi_c(T)\sim d/2$].[3]

Maki and Thompson[12] considered a theory that an additional contribution to the paraconductivity arises from enhancement of the normal-state conductivity by the superconducting fluctuations in the presence of the pair-breaking effects. This process is limited by strong inelastic scattering and by the other pair-breaking interactions, such as magnetic impurities or intrinsic magnetic moments. The MT contribution to paraconductivity has the following forms in the 2D and 3D systems:

$$(\Delta\sigma_{xx}^{\mathrm{MT}})_{3\mathrm{D}}=\frac{e^2}{8\hbar d}\frac{1}{\xi_c(0)}\varepsilon^{-1/2} \tag{5}$$

and

$$(\Delta\sigma_{xx}^{\mathrm{MT}})_{2\mathrm{D}}=\frac{e^2}{8\hbar d}\frac{1}{(\varepsilon-\delta)}\ln\left(\frac{\varepsilon}{\delta}\right), \tag{6}$$

where a pair-breaking parameter $\delta=\pi\hbar/8k_BT\tau_\phi$ is introduced and τ_ϕ is the phase-relaxation time of the quasiparticle.[24]

Furthermore, the MT model has been recently extended to layered superconductors by Maki and Thompson as a function of temperature, external magnetic field, and internal pair breaking.[25]

$$\Delta\sigma_{xx}^{\mathrm{MT}}=\frac{e^2}{16\hbar d}\frac{2}{\varepsilon-\delta}\ln\left\{\frac{\varepsilon}{\delta}\frac{1+\alpha+(1+2\alpha)^{1/2}}{1+\alpha\varepsilon/\delta+(1+2\alpha\varepsilon/\delta)^{1/2}}\right\}. \tag{7}$$

Recently, Lang *et al.*[3] reported that a better fit for the fluctuation-enhanced conductivity data in the YBCO film was obtained by adding a MT contribution to the LD model. Thus $\Delta\sigma_{xx}=\Delta\sigma_{xx}^{\mathrm{LD}}+\Delta\sigma_{xx}^{\mathrm{MT}}$ is considered in this study of paraconductivity.

B. Excess Hall effect

The studies of the fluctuation Hall effect by Abrahams *et al.*[26] and by Fukuyama *et al.*[27] were based on the time-dependent Ginzburg-Landau (TDGL) equation in a microscopic, BCS-based calculation. Fukuyama *et al.* considered both the AL and MT contributions to the excess Hall conductivity $\Delta\sigma_{xy}$ and found that the MT process yields a positive contribution, whereas the AL term may be either positive or negative. More recently, Ullah and Dorsey[9] (UD) presented a theory that reproduced the results of Fukuyama *et al.* and calculated the temperature dependence of the AL term in $\Delta\sigma_{xy}$ for the layered-structure model. In the low-field limit, they found

$$\Delta\sigma_{xy}^{\mathrm{AL}}=\frac{e^2}{16\hbar d}\frac{\sigma_{xy}^N}{\sigma_{xx}^N}\beta\frac{\pi d}{72\xi_c(0)}\frac{1+1/\alpha}{(1+1/2\alpha)^{3/2}}\varepsilon^{-3/2}, \tag{8}$$

where $\Delta\sigma_{xx}^N$ and $\Delta\sigma_{xy}^N$ are the normal-state longitudinal conductivity and Hall conductivity, respectively. The parameter β is considered as the imaginary part of the relaxation rate in the TDGL equation that reflects the sign of the AL contributions.[9]

For the MT contribution, the MT process for the excess Hall effect also scales with the MT paraconductivity contribution:[3]

$$\Delta\sigma_{xy}^{\mathrm{MT}}=2(\sigma_{xy}^N/\sigma_{xx}^N)\Delta\sigma_{xx}^{\mathrm{MT}}, \tag{9}$$

in the derived region. Associating Eq. (7) with Eq. (9), the formula

$$\Delta\sigma_{xy}^{\mathrm{MT}}=\frac{e^2}{16\hbar d}\frac{\sigma_{xy}^N}{\sigma_{xx}^N}\frac{4}{\varepsilon-\delta}\ln\left\{\frac{\varepsilon}{\delta}\frac{1+\alpha+(1+2\alpha)^{1/2}}{1+\alpha\varepsilon/\delta+(1+2\alpha\varepsilon/\delta)^{1/2}}\right\} \tag{10}$$

is induced, and finally the excess Hall effect is $\Delta\sigma_{xy}=\Delta\sigma_{xy}^{\mathrm{AL}}+\Delta\sigma_{xy}^{\mathrm{MT}}$.

C. Scaling functions of $\Delta\sigma_{xx}$ and $\Delta\sigma_{xy}$

The presence of a strong magnetic field raises the complexity of the analysis of fluctuation conductivity. The quantity $\varepsilon=(T-T_c)/T_c$ not only strongly depends on the temperature, but also on the magnitude of magnetic fields. Based on the framework of the AL models, both $\Delta\sigma_{xx}(H)$ and $\Delta\sigma_{xy}(H)$ can be expressed in the following scaling forms for a 2D or 3D system:[17,28,29]

$$\Delta\sigma(H)_{2D}=\left[\frac{T}{H}\right]^{1/2} f_{2D}\left[A\frac{T-T_c(H)}{(TH)^{1/2}}\right] \quad \text{for a 2D system} \tag{11}$$

and

$$\Delta\sigma(H)_{3D}=\left[\frac{T^2}{H}\right]^{1/3} f_{3D}\left[B\frac{T-T_c(H)}{(TH)^{2/3}}\right] \quad \text{for a 3D system.} \tag{12}$$

Here A and B are appropriate constants characterizing the materials, and f_{2D} and f_{3D} are unspecified scaling functions.

Ullah and Dorsey[9] calculated similar transport properties of a superconductor near T_c in a magnetic field and obtained scaling forms similar to Eq. (12). They also introduced the anisotropy parameter in the three-dimensional systems and found that the high-field conductivity has a scaling form

$$(\Delta\sigma_{xx}^{\mathrm{UD}})_{3D}=C_{xx}\gamma^{1/3}\left[\frac{T^2}{H}\right]^{1/3} f_{3D}\left[\frac{\gamma^{2/3}[T-T_c(H)]}{(HT)^{2/3}T_c(H)}\right], \tag{13}$$

where $\gamma=[\xi_c(0)/\xi_{ab}(0)]^2$ and C_{xx} is related to the real part of the relaxation rate Γ_0^{-1} in the TDGL equation. Furthermore, Ullah and Dorsey pointed out that the scaling functions for the high field $\Delta\sigma_{xy}$ are the same as $\Delta\sigma_{xx}$, apart from the replacement of Γ_0^{-1} by λ_0^{-1} where λ_0^{-1} is the imaginary part of the relaxation rate.

III. ANALYSIS AND DISCUSSION

A. Paraconductivity

Above T_c, the conductivity σ_{xx} is composed of contributions from the normal state and superconducting fluctuations, σ_{xx}^N and $\Delta\sigma_{xx}$, respectively, and $\sigma_{xx}=\sigma_{xx}^N+\Delta\sigma_{xx}$. For the evaluation of $\Delta\sigma_{xx}$, the normal-state conductivity σ_{xx}^N has to be subtracted from the measured quality. We determine σ_{xx}^N by extrapolating the linear part of each $\rho_{xx}(T)$ curve (120–210 K) to the fluctuation region as indicated in the inset of Fig. 1. This approach is commonly used in the study of $\Delta\sigma_{xx}$ in high-T_c superconductors. Although it is possible to determine ρ_{xx}^N by taking other approaches, e.g., the size-effect contribution[30,31] to the resistivity, however, a better fit to the experimental data is not obtained by taking other approaches.

We first fitted the fluctuation conductivity of the YBCO films and YBCO/PBCO (120 Å/96 Å) superlattice $\Delta\sigma_{xx}$ in zero magnetic field by AL theory. As predicted by AL theory, there is a crossover from 2D to 3D as the temperature is reduced to T_c. However, we find that the 3D and 2D fits did not yield good agreement within the temperature investigated. This result implies that the paraconductivities of YBCO films and YBCO/PBCO superlattices can not be well described by 3D or 2D AL theory. Second, the data were fitted to the LD model. As shown in Fig. 1, the 2D AL term separated from the LD term is the dashed line. It is found that the 2D AL term deviates from the LD term (solid line) at $\varepsilon<0.03$ and at $\varepsilon<0.08$ for the YBCO/PBCO (120 Å/96 Å) superlattice and YBCO films, respectively. This result is consistent with the inference that the LD form would reduce to the 3D AL form at temperatures near T_c and results in the deviation between the LD and 2D AL fittings at lower values of ε. However, the LD theory fit the experimental data only within a range of $0.03<\varepsilon<0.1$, indicating that an additional contribution should be considered.

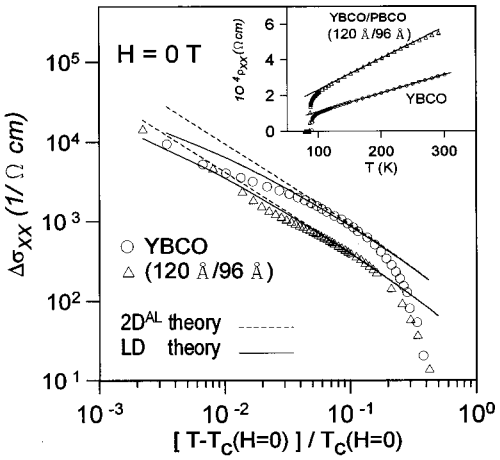

FIG. 1. Paraconductivity of YBCO and YBCO/PBCO (120 Å/96 Å) superlattices as a function of ε, where $\varepsilon=(T-T_c)/T_c$. The solid lines represent the results from the fit of LD theory, while the dashed lines represent the 2D AL term separated from the LD term. The inset shows the temperature dependence of the resistivity ρ_{xx}. The ρ_{xx}^N is determined by extrapolating the linear part of the $\rho_{xx}(T)$ curve to fluctuation region.

Recently, Solovjov *et al.*[32] analyzed the fluctuation conductivity $\Delta\sigma_{xx}$ of YBCO/PBCO superlattices and found a clear LD-MT crossover for some samples. For our samples, the LD-MT-like crossover also could be observed in this analysis and was strongly dependent on the selected values of $T_c(H=0)$. However, we cannot simultaneously get a good fit for the LD term and MT term individually in the lower- and higher-temperature regions, respectively. Finally, we adopt the analyses including both LD and MT contributions. The paraconductivity $\Delta\sigma_{xx}$ along with the values fitted from Eqs. (3) and (7) are plotted in Fig. 2 and its inset for the YBCO/PBCO (120 Å/96 Å) superlattice and YBCO films, respectively. There are three adjustable parameters $\xi_c(0)$, δ,

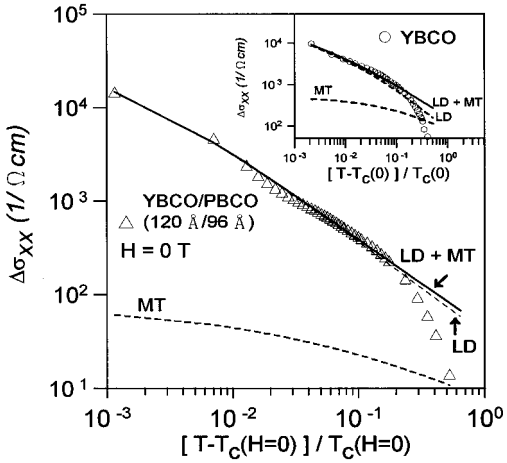

FIG. 2. Paraconductivity of the YBCO/PBCO (120 Å/96 Å) superlattice and YBCO film (shown in the inset) as a function of ε. The dashed lines represent the results deduced from the fit of the LD and MT fluctuation processes separately. The sum of these two contributions (LD+MT) is represented by the solid line.

TABLE I. Values of parameters used in the $\Delta\sigma_{xx}(H=0)$ fit. The values of $T_c(50\%)$, $\xi_c(0)$, $\xi_{ab}(0)$, and γ obtained by resistive transitions and measurements on the critical field H_{c2} are also shown. It is noted that in the $(\Delta\sigma_{xx}^{\mathrm{LD}}+\Delta\sigma_{xx}^{\mathrm{MT}})$ fitting, the parameter d is taken as d_{PBCO} for YBCO/PBCO superlattices and 11.7 Å for the YBCO film.

	$\Delta\sigma_{xx}^{\mathrm{LD}}+\Delta\sigma_{xx}^{\mathrm{MT}}$				Measured			
Samples (YBCO/PBCO)	$\xi_c(0)$ (Å)	δ	$T_c(H=0)$ (K)	$\tau_\phi(100\,\mathrm{K})$ $(10^{-14}\,\mathrm{s})$	$T_c(50\%)$ (K)	$\xi_c(0)$ (Å)	$\xi_{ab}(0)$ (Å)	γ
(36 Å/24 Å)	1.93	0.454	81.51	6.61	83.81	1.56	24.3	0.0041
(36 Å/48 Å)	1.12	0.380	74.77	7.89	79.69	0.86	26.3	0.0011
(36 Å/60 Å)	0.94	0.381	71.05	7.87	78.83	0.78	27.3	0.0008
(36 Å/72 Å)	0.93	0.365	66.35	8.22	73.96	0.64	30.5	0.0004
(36 Å/96 Å)	0.92	0.452	61.34	6.64	68.68	0.77	32.4	0.0006
(96 Å/60 Å)	3.34	0.362	85.36	8.29	85.83	2.86	22.0	0.0170
(60 Å/60 Å)	2.70	0.356	82.82	8.43	84.09	2.06	22.4	0.0085
(48 Å/60 Å)	1.35	0.359	78.83	8.36	80.91	0.95	26.9	0.0013
(36 Å/60 Å)	0.94	0.381	71.05	7.87	78.83	0.78	27.3	0.0008
(120 Å/96 Å)	3.18	0.421	85.93	7.13	86.33	2.53	21.4	0.0139
YBCO film	2.45	0.301	89.37	9.97	89.43	3.11	20.2	0.0237
YBCO film (Ref. 3)	1.50	0.35	88.55	8.6				
YBCO single crystal (Ref. 1)	2.4	0.01	94.35	300				
Superlattices (Ref. 30)	1.5–1.7	0.11–0.43	82.4–87.9	7–27				

and $T_c(H=0)$, while d is taken by the thickness of the PBCO layers and by 11.7 Å for YBCO films. The sum of these two contributions (LD+MT) is also displayed in Fig. 2.

As shown in Fig. 2, the theories including LD and MT processes can fit to the experimental data well for a larger range of $0.001<\varepsilon<0.2$ than that shown in Fig. 1. The results shown in Fig. 2 also indicate that in the fitted range, the paraconductivity is governed by the LD contribution. These results imply that beside the contribution due to the layered superconductors, an additional contribution to the paraconductivity due to the MT process should be small in the YBCO/PBCO superlattice systems. The small MT contribution also implies that an intrinsic inelastic scattering or pair-breaking interaction exists in the superlattice systems even in a zero field. Similar results are obtained for the $\Delta\sigma_{xx}$ data of other YBCO/PBCO superlattices.

From these fitting procedures, the resulting parameters are listed in Table I. As we see in Table I, the fitted values of critical temperature $T_c(H=0)$ are close to the point of the 50% resistive transition. The estimated values of phase-relaxation time $\tau_\phi(100\,\mathrm{K})$ are also shown in Table I. As results, the value $\tau_\phi(100\,\mathrm{K})=6.61-8.43\times10^{-14}\,\mathrm{s}$ for all superlattices studied is smaller than that $\tau_\phi(100\,\mathrm{K})=9.97\times10^{-14}\,\mathrm{s}$ obtained in the YBCO film. The observed lower τ_ϕ for YBCO/PBCO superlattices is attributable to the influence of additional interaction via PBCO stacks. The samples parameters of single-crystal YBCO, YBCO film, and YBCO/PBCO superlattices, which are obtained by other workers, are listed in Table I also. The values of the phase-relaxation time measured on our YBCO films or superlattices are comparable with that obtained by other workers. However, the values of τ_ϕ at $T=100\,\mathrm{K}$ from each of our fits are 0.02–0.03 times smaller than ~3 ps of single-crystal YBCO.[30] This might reflect that some defects or structure inhomogeneity will give rise to some additional scattering in the YBCO films and superlattices. Additionally, as shown in Table I, the derived *c*-axis coherence length is close to that estimated from our resistive measurements. This deviation may be possibly due to the larger d values taken by the thickness of the PBCO layers. In fact, the effective d values should be smaller than the thickness of the PBCO layers owing to superconducting coupling between the neighboring YBCO layers.

B. Excess Hall effect

The excess Hall effect is an additional contribution to the Hall conductivity,

$$\sigma_{xy}=\rho_{xy}/(\rho_{xx}^2+\rho_{xy}^2)\approx\rho_{xy}/\rho_{xx}^2, \tag{14}$$

and the total Hall conductivity σ_{xy} may be expressed as

$$\sigma_{xy}=\sigma_{xy}^N+\Delta\sigma_{xy}, \tag{15}$$

where σ_{xy}^N is the normal-state Hall conductivity and $\Delta\sigma_{xy}$ is the excess Hall conductivity. For an evaluation of $\Delta\sigma_{xy}$, we must subtract the normal-state contribution σ_{xy}^N. The nature of the temperature dependence of the Hall effect in the normal state for our samples has been discussed elsewhere.[22] It has been shown that, in fact, many measurements on the Hall conductivities of the high-T_c superconductors may be explained in terms of the Anderson's formula[33]

$$\cot\theta_H^N=AT^2+B. \tag{16}$$

From Eqs. (14) and (16), we obtain the Hall conductivity in the normal state:

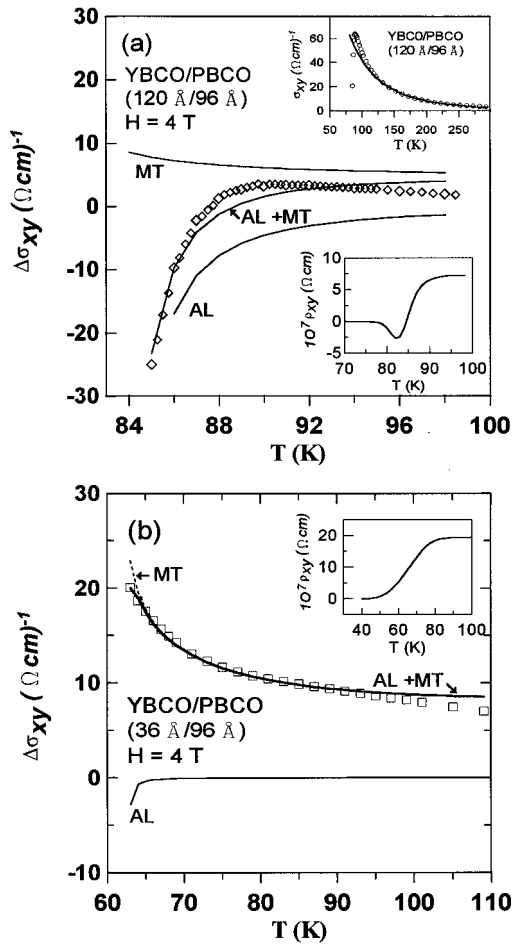

FIG. 3. Excess Hall effect $\Delta\sigma_{xy}$ of (a) YBCO/PBCO (120 Å/96 Å) and (b) YBCO/PBCO (36 Å/96 Å) superlattices as a function of the temperature. The line labeled AL+MT is the result calculated by the fit to the sum of the AL and MT fluctuation contributions, which are also shown separately. Insets show the corresponding Hall resistivities for both samples. The upper panel in (a) shows the Hall conductivity σ_{xy} as a function of the temperature T. The solid line presents the normal-state Hall conductivity σ_{xy}^{N}. Deviation from this line is interpreted as fluctuation contributions to the Hall effect.

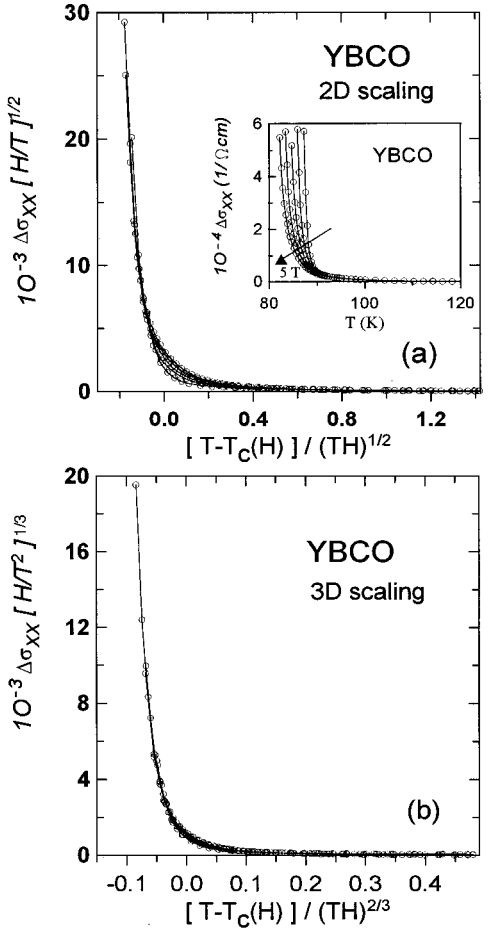

FIG. 4. Scaling plots in the (a) 2D and (b) 3D models of the excess conductivity $\Delta\sigma_{xx}$ vs temperature for a YBCO film in magnetic fields $H=1$, 2, 3, 4, and 5 T parallel to the c axis. The inset shows the corresponding fluctuation conductivity.

$$\sigma_{xy}^{N}=(\rho_{xx}^{N}\cot\theta_{H}^{N})^{-1}. \tag{17}$$

In the inset of Fig. 3(a), we compare the σ_{xy} determined from the measurements of the Hall effect with the normal-state Hall conductivity, σ_{xy}^{N}, for the YBCO/PBCO (120 Å/96 Å) superlattice. At temperatures below 120 K, σ_{xy} begins to exceed the values expected from the normal-state extrapolation, exhibiting a local maximum at around 92 K, and falling below σ_{xy}^{N} at lower temperatures. This behavior clearly indicates two different, offsetting contributions with different temperature dependences. One of the contributions reduces σ_{xy}, becoming dominant only when it is close to the superconducting transition and exhibiting a negative σ_{xy} at lower temperatures.

Now we compare the excess Hall effect $\Delta\sigma_{xy}$ to the theoretical predictions based on Eqs. (8) and (10). There is only one adjustable parameter β and the same parameters $\xi_c(0)$, T_c, and δ for the paraconductivity are used. In Fig. 3(a), we show $\Delta\sigma_{xy}$ of the YBCO/PBCO (120 Å/96 Å) superlattice along with the AL and MT contributions calculated from the fit, using $\beta\approx-0.075$. The sum of the two fluctuations process (AL+MT) yields a better fit to the experimental data with a sign change around 86 K being included. A similar behavior is observed for a YBCO film where a sign change occurs around 89 K. It is noteworthy that the contribution $\Delta\sigma_{xy}^{\mathrm{MT}}$ is positive and dominates at higher temperatures. Otherwise, a negative contribution from the AL process is observed, which governs $\Delta\sigma_{xy}$ close to T_c. The results are obviously different from those observed in paraconductivity which the LD term (AL process) governs even close to T_c. The small β value ($|\beta|\ll 1$) also deduces a smaller value of λ_0^{-1} [i.e., $\Delta\sigma_{xy}^{\mathrm{AL}}\ll\Delta\sigma_{xy}^{\mathrm{MT}}$, while $\Delta\sigma_{xx}^{\mathrm{LD}}(\mathrm{AL\ process})\gg\Delta\sigma_{xx}^{\mathrm{MT}}$] and reflects an asymmetry between the real (Γ_0^{-1}) and imaginary (λ_0^{-1}) parts of the relaxation rate in the TDGL equation, since the parameters Γ_0^{-1} and λ_0^{-1} introduced by UD theory[9] (AL process) are proportional to the contributions to the paraconductivity and excess Hall conductivity, respectively.

However, is the property of excess Hall conductivity observed in the YBCO films and YBCO/PBCO (120 Å/96 Å) superlattices a common feature in all the superlattices? A different result is shown in Fig. 3(b) for the YBCO/PBCO

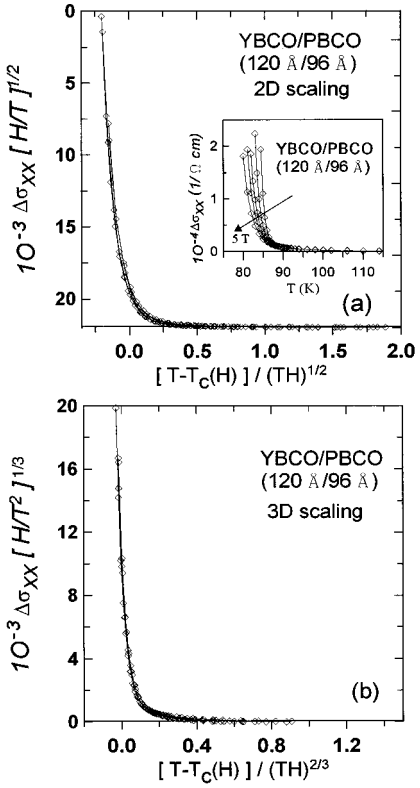

FIG. 5. Scaling plots in the (a) 2D and (b) 3D models of the excess conductivity $\Delta\sigma_{xx}$ vs temperature for the YBCO/PBCO (120 Å/96 Å) superlattice in magnetic fields $H=1$, 2, 3, 4, and 5 T parallel to the c axis. The inset shows the corresponding fluctuation conductivity.

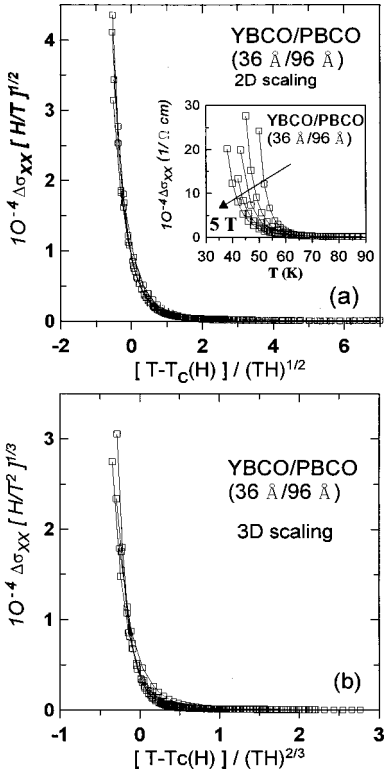

FIG. 6. Scaling plots in the (a) 2D and (b) 3D models of the excess conductivity $\Delta\sigma_{xx}$ vs temperature for the YBCO/PBCO (36 Å/96 Å) superlattice in magnetic fields $H=1$, 2, 3, 4, and 5 T parallel to the c axis. The inset shows the corresponding fluctuation conductivity.

(36 Å/96 Å) superlattices. In this case, the contribution $\Delta\sigma_{xy}^{\mathrm{MT}}$ dominates within the temperatures investigated. The contribution $\Delta\sigma_{xy}^{\mathrm{AL}}$ is small and negative due to a smaller adjustable parameter $\beta\approx-0.0003$ used for the YBCO/PBCO (36 Å/96 Å) superlattice.

As expected from the above results, it is speculated that this negative fluctuation Hall effect may exceed the positive normal-state Hall effect as approaching T_c from the high-temperature side for the YBCO films or YBCO/PBCO (120 Å/96 Å) superlattice. This negative contribution leads to the reduction of the Hall conductivity and consequently the negative Hall resistivity ρ_{xy} in the mixed state as shown in the lower inset of Fig. 3(a). For the YBCO/PBCO (36 Å/96 Å) superlattice, with a lower T_c, a lower H_{c2}, and a high-anisotropy layered structure, we do not observe a sign change of ρ_{xy}, even down to the superconducting state [see the inset of Fig. 3(b)]. However, it may be noted that a negative contribution possibly exists in the Hall conductivity, although this contribution is very small. Additionally, the MT term dominating the contribution of $\Delta\sigma_{xy}$ in the YBCO/PBCO (36 Å/96 Å) superlattice implies that the strong inelastic scattering and pair-breaking interaction are important in this sample. The positive MT contribution may be taken as a role that diminishes the sign reversal. However, we also note that the fluctuation effect in the critical regime interpolates smoothly between the fluctuation region above $T_c(H)$ and the flux-flow region below. The negative Hall effect in the flux-flow region has been previously explained in the framework of vortex-motion theories.[34,35] Thus a negative fluctuation Hall effect $\Delta\sigma_{xy}$ means that the Hall conductivity σ_{xy} is reduced as T is close to T_c and is related to a sign change of the Hall effect in the mixed state. Contrariwise, a large positive fluctuation $\Delta\sigma_{xy}$ will diminish the sign change of ρ_{xy} as $T>T_c(H)$. However, in previous work,[20] the diminishing of the anomalous Hall effect in the mixed-state region has been attributed to the weak pinning of flux. Associating the present analyses with the results of the previous work, we can infer that the reduction of ρ_{xy} is governed by the fluctuation conductivity $\Delta\sigma_{xy}^{\mathrm{AL}}$ at temperature above $T_c(H)$, while the negative Hall resistivity in the mixed state is strongly dependent on the pinning as $T<T_c(H)$. The consistency also could be realized by the reason that the pair-breaking effect and the inelastic scattering may reduce the pinning ability.

C. Scaling of $\Delta\sigma_{xx}(H)$ and $\Delta\sigma_{xy}(H)$

In the presence of magnetic fields, the contribution of the MT-term conductivity is strongly depressed by the pair-breaking effect, and the dimensionality can then be well examined in the fluctuation region using the 2D [Eq. (11)] and 3D [Eq. (12)] scaling functions which are based on the AL model. Three samples, the YBCO thin film and the YBCO/PBCO (120 Å/96 Å) and (36 Å/96 Å) superlattices were investigated, in which the anisotropy parameters (m_{ab}/m_c) are about 0.0237, 0.0139, and 0.0006, respectively.

The most important parameter in Eqs. (11) and (12) is to determine the mean-field transition temperature in the pres-

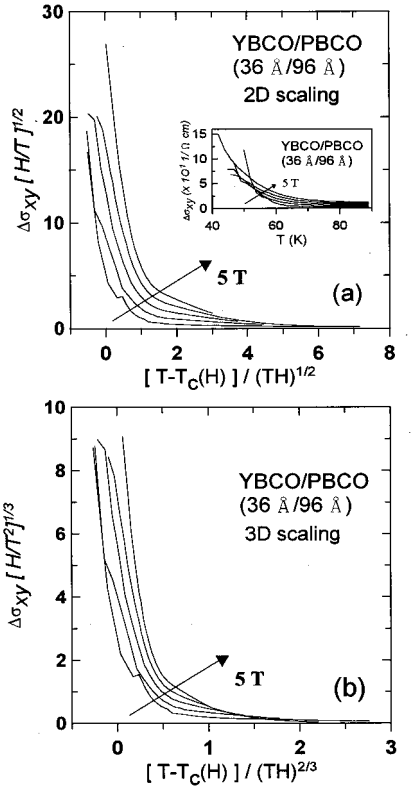

FIG. 7. Scaling plots in the (a) 2D and (b) 3D models of the excess Hall conductivity $\Delta\sigma_{xy}$ vs temperature for the YBCO/PBCO (36 Å/96 Å) superlattice in magnetic fields $H=1$, 2, 3, 4, and 5 T parallel to the c axis. The inset shows the corresponding fluctuation conductivity in the unscaled plots.

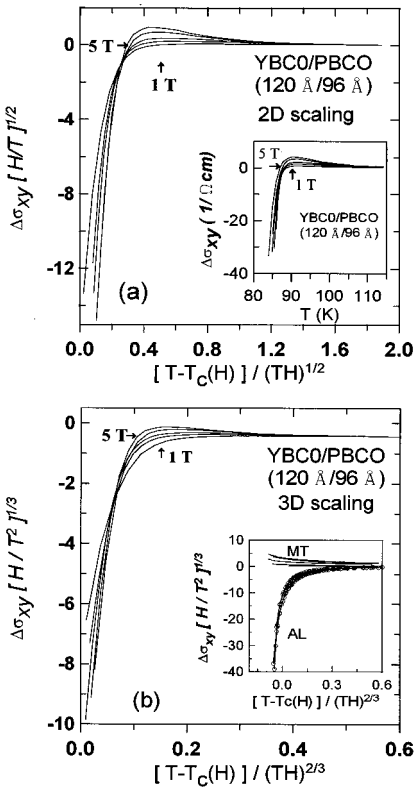

FIG. 8. Scaling plots in the (a) 2D and (b) 3D models of the excess Hall conductivity $\Delta\sigma_{xy}$ vs temperature for the YBCO/PBCO (120 Å/96 Å) superlattice in magnetic fields $H=1$, 2, 3, 4, and 5 T parallel to the c axis. Insets show the corresponding fluctuation conductivity (a) and the 3D-scaling plots of AL and MT Hall conductivities (b).

ence of a magnetic field, $T_c(H)$. According to Ginzburg-Landau theory, the shift is described by

$$\ln\left[\frac{T_{c0}}{T_c(H)}\right]\approx\frac{T_{c0}-T_c(H)}{T_c(H)}=\frac{H}{T_c(H)}\left[\frac{dH_{c2}}{dT}\right]^{-1}_{T_{c0}},$$

where the values of T_{c0} and dH_{c2}/dT can be well determined from the fluctuation fit and the resistive measurements.

Figures 4(a) and 4(b) show the scaling plots for a YBCO film in the 2D and 3D models, respectively. The inset of Fig. 4(a) also shows the excess conductivity $\Delta\sigma_{xy}$ vs temperature for a YBCO film in magnetic fields $H=1$, 2, 3, 4, and 5 T parallel to the c axis. It is notable that the scaling is very sensitive to the choice of values for T_{c0}. We find that the best fit is obtained by $T_{c0}\approx T_c(R\approx 0)$ for all samples investigated. The scaling of 2D formula remains poor for a YBCO film. Furthermore, as shown in Fig. 4(b), the data points for different fields merge and follow at one curve, indicating that the scaling of 3D formula seems to be a better fit than that shown in Fig. 4(a).

Similar results are obtained for the YBCO/PBCO (120 Å/96 Å) superlattice. The 2D and 3D scaling plots of $\Delta\sigma_{xx}$ for the YBCO/PBCO (120 Å/96 Å) superlattice are shown in Figs. 5(a) and 5(b), respectively. Similar to the data for a YBCO film, the 3D scaling seems to fit well for the YBCO/PBCO (120 Å/96 Å) superlattice. It implies that the dimensionalities of the YBCO/PBCO (120 Å/96 Å) superlattices and YBCO films tend to be 3D within the fluctuation region. The dimensionalities are clear and different from that revealed in the zero-field (LD+MT) fits. The difference can be realized by the reason that the paraconductivities of MT terms are depressed, i.e., limited by the pair-breaking effect in the presence of magnetic fields, and then the dimensionalities are more consistent with the prediction of the scaling theories based on the AL process.

For the YBCO/PBCO (36 Å/96 Å) superlattice, although a quasi-two-dimensional behavior might have been expected because of the small γ value, we obtain a better fit for 2D scaling [Fig. 6(a)] than for 3D scaling [Fig. 6(b)] in $\Delta\sigma_{xx}$. According to the scaling of the paraconductivity of the YBCO film and YBCO/PBCO (120 Å/96 Å) and (36 Å/96 Å) superlattices, it is recognized that the dimensionality of the YBCO/PBCO superlattices is not exactly 2D or 3D, since it is a quasi-2D system. The anisotropy parameter γ could correspond to dimensionality ($\gamma=0$ for 2D and $\gamma=1$ for 3D) within the fluctuation scaling. For a larger γ value, a 3D-like tendency is expected in the YBCO film or YBCO/PBCO superlattices with thicker YBCO layers. The successful 3D scaling for the YBCO film and YBCO/PBCO (120 Å/96 Å) superlattice indicates the strong-coupling effect that occurs in them.

Ullah and Dorsey also pointed out that the scaling functions for $\Delta\sigma_{xy}$ are the same as those for $\Delta\sigma_{xx}$, apart from the replacement of Γ_0^{-1} by λ_0^{-1}. Therefore, we can fit the data for $\Delta\sigma_{xy}$ of YBCO/PBCO (120 Å/96 Å) and YBCO/

PBCO (36 Å/96 Å) superlattices using the same scaling functions as shown in Figs. 7 and 8, respectively. It is obvious that Figs. 7(a) and 7(b) do not show agreement with the scaling functions for the excess Hall conductivity of YBCO/PBCO (36 Å/96 Å) superlattices. Recently, Liu *et al.*[21] reported that the AL Hall conductivity follows a scaling fit in their YBCO film, while the MT Hall conductivity does not. They separated the AL term from the total fluctuation conductivity by adjusting a numerical factor, which corresponds to the relative strength between AL and MT terms to achieve a nice scaling for the AL Hall conductivity. In the inset of Fig. 8(b), we perform a 3D-scaling plot of the AL Hall conductivity of the YBCO/PBCO (120 Å/96 Å) superlattice. Notably, using a method different from that used in the work of Liu *et al.*, we could separate the AL and MT terms from the total Hall conductivities as in previous analyses for the excess Hall effect; i.e., we used the sum of $\Delta\sigma_{xy}^{\mathrm{AL}}$ [Eq. (8)] and $\Delta\sigma_{xy}^{\mathrm{MT}}$ [Eq. (10)] to make a direct theoretical fitting. In the inset of Fig. 8(b), it can be seen that the 3D-scaling plots of the AL Hall conductivity show a nice scaling, while the 3D-scaling plots of the MT term do not. According to this result, the poor scaling plots shown in Figs. 7(a) and 7(b) are obtained. We cannot obtain a nice scaling in Fig. 7 owing to the MT-dominating Hall conductivity of YBCO/PBCO (36 Å/96 Å) superlattice as analyzed previously. This failure to scale also could be deduced by the fact that the TDGL scaling theory only includes AL contributions, but fails to include MT contributions.

IV. CONCLUSION

We have presented measurements on the resistivity and Hall effect of YBCO films and YBCO/PBCO superlattices in the fluctuation region. The paraconductivity and excess Hall effect observed in a limited temperature range above T_c are interpreted as additional contributions from thermodynamic fluctuations of the superconducting order parameter.

The data are analyzed in terms of the theories for layered superconductors, including the LD (or AL) and MT contributions. We find that the LD process governs the fluctuations of the paraconductivity, although the MT term possibly dominates the fluctuation contributions to the excess Hall effect in the YBCO/PBCO superlattices with a thinner thickness of YBCO layers. Especially, for the excess Hall effect of YBCO/PBCO (36 Å/96 Å) superlattices, the positive MT term dominates the fluctuation contributions accompanying a weak pinning and may result in a diminished sign reversal of the Hall effect.

The excess conductivities $\Delta\sigma_{xx}(H)$ and $\Delta\sigma_{xy}(H)$ are also analyzed with the 2D and 3D scaling forms. In the presence of magnetic fields, the dimensionality is more clear due to the depression and the small contribution of the MT contributions. For the paraconductivity of the YBCO films or YBCO/PBCO (120 Å/96 Å) superlattice, with a larger value of γ, the dimensionality shows a strong 3D tendency in the scaling analyses. The results suggest that the dimensionality of the superlattice belongs to a quasi-2D system and the parameter γ governs the dimensionality. Additionally, we can separate the AL Hall conductivity from the total conductivity with a theoretical fitting and achieve a better scaling for the AL Hall conductivity. The failure to scale the excess Hall conductivity is due to the MT contributions, which the scaling theory does not include.

ACKNOWLEDGMENT

The authors thank the National Science Council of the Republic of China for financial support under Grant No. NSC 87-2112-M002-031.

[1] J. P. Rice, J. Giapintzukis, D. M. Ginsberg, and J. M. Mochel, Phys. Rev. B **44**, 10 158 (1991).
[2] A. V. Samoilov, Phys. Rev. B **49**, 1246 (1994).
[3] W. Lang, G. Heine, P. Schwab, X. Z. Wang, and D. Bäuerle, Phys. Rev. B **49**, 4209 (1994).
[4] A. K. Pardhan, S. B. Roy, P. Chaddah, C. Chen, and B. M. Wanklyn, Phys. Rev. B **50**, 7180 (1994).
[5] V. Calzona, M. R. Cimberle, C. Ferdeghini, G. Grasso, D. V. Livamov, D. Marre, M. Putti, and A. S. Siri, Solid State Commun. **87**, 397 (1993).
[6] E. Inderhees, M. B. Salamon, J. P. Rice, and D. M. Ginsberg, Phys. Rev. Lett. **66**, 232 (1991).
[7] W. L. Lee, R. A. Klemm, and D. C. Johnston, Phys. Rev. Lett. **63**, 1012 (1989).
[8] Y. Matsuda, T. Hirai, S. Komiyama, T. Terashima, Y. Bando, K. Iijima, K. Yamamoto, and K. Hirata, Phys. Rev. B **40**, 5176 (1989).
[9] Salman Ullah and Alan T. Dorsey, Phys. Rev. B **44**, 262 (1991).
[10] Kazumi Maki and R. S. Thompson, Phys. Rev. B **39**, 2767 (1989).
[11] L. G. Aslamazov and A. I. Larkin, Sov. Phys. Solid State **10**, 875 (1968).
[12] K. Maki, Prog. Theor. Phys. **39**, 897 (1968); R. S. Thompson, Phys. Rev. B **1**, 327 (1970).
[13] N. P. Ong, Z. Z. Wang, S. Hagen, T. W. Jing, and J. Hovarth, Physica C **153-155**, 1072 (1988).
[14] S. Martin, A. T. Fiory, R. M. Fleming, L. F. Schneemeyer, and V. J. Wasczak, Phys. Rev. Lett. **60**, 2194 (1988).
[15] D. H. Kim, A. M. Goldman, J. H. Kang, K. E. Gray, and R. T. Kampwirth, Phys. Rev. B **39**, 12 275 (1989).
[16] D. H. Kim, K. E. Gry, and M. D. Trochet, Phys. Rev. B **45**, 10 801 (1992).
[17] S. Ullah and A. T. Dorsey, Phys. Rev. Lett. **65**, 2066 (1991).
[18] Z. Tesanovic, L. Xiang, L. Bulaevskii, Q. Li, and M. Sucnaga, Phys. Rev. Lett. **69**, 3563 (1992).
[19] Kebin Li, Y. Zhang, and H. Adrian, Phys. Rev. B **53**, 8608 (1996).
[20] L. M. Wang, H. C. Yang, and H. E. Horng, Phys. Rev. Lett. **78**, 527 (1997).
[21] Wu Liu, T. W. Clinton, A. W. Smith, and C. J. Lobb, Phys. Rev. B **55**, 11 802 (1997).
[22] L. M. Wang, H. C. Yang, and H. E. Horng, Phys. Rev. B **56**, 6231 (1997).
[23] W. E. Lawrence and S. Doniach, in *Proceedings of the Twelfth*

International Conference on Low Temperature Physics, Kyoto, 1970, edited by Eizo Kanda (Keigaku, Tokyo, 1971), p. 361.
[24] B. R. Patton, Phys. Rev. Lett. **27**, 1273 (1971).
[25] K. Maki and R. S. Thompson, Phys. Rev. B **39**, 2767 (1989).
[26] E. Abrahams, R. E. Drange, and M. J. Stephen, Physica (Amsterdam) **55**, 230 (1971).
[27] H. Fukuyama, H. Ebisawa, and T. Tsuzuki, Prog. Theor. Phys. **46**, 1028 (1971).
[28] A. T. Dorsey, Phys. Rev. B **46**, 8376 (1992).
[29] A. G. Aronov and S. Hikami, Phys. Rev. B **41**, 9548 (1990).
[30] A. L. Solovjov, H.-U. Jabermeier, and I. E. Trofimov, Physica B **199 & 200**, 260 (1994).
[31] Guoliang Liu, Guangcheng Xiong, Guohong Li, Cuijum Lian, Ke Wu, Sangtian Liu, Jie Li, and Shousheng Yan, Phys. Rev. B **49**, 15 287 (1994).
[32] A. L. Solovjov, V. M. Dmitriev, H. U. Habermeier, and I. E. Trofimov, Phys. Rev. B **55**, 8551 (1997).
[33] P. W. Anderson, Phys. Rev. Lett. **67**, 2092 (1991).
[34] S. J. Hagen, C. J. Cobb, R. L. Greone, M. G. Forester, and J. H. Kang, Phys. Rev. B **41**, 11 630 (1990).
[35] Z. D. Wang, Jiming Dong, and C. S. Ting, Phys. Rev. Lett. **72**, 3875 (1994).